Journal of Spacecraft and Rockets

VOLUME 7 OCTOBER 1970 NUMBER 10

Axisymmetric Vibration of Conical Shells

R. F. Hartung* and W. A. Loden†
Lockheed Palo Alto Research Laboratory, Palo Alto, Calif.

The axisymmetric modal properties (frequencies and mode shapes) of thin conical shell frusta are studied to determine how they are influenced by the cone length, thickness, apex angle, and boundary conditions. Shear deformation and rotatory inertia effects are not considered. In portions of the frequency spectrum, the cone is observed to vibrate vigorously at the large end while the small end remains relatively quiescent. The paper contains numerous graphs and illustrations obtained while examining some 3000 different configurations. Results were obtained using a computer program based on a finite element analysis in which the cone is treated as an assemblage of conical frusta. Details of the computer program are not presented in the paper as they have been reported elsewhere.

Introduction

THE structural design of a typical aerospace vehicle requires that the response of the vehicle to various mission-dictated excitations be accurately predicted so that the integrity of the vehicle and its contents can be assessed. To this end, a thorough understanding of the natural modes of the vehicle is extremely helpful, if not essential. The conical shell is extensively used as a structural component in many existing and proposed flight vehicles. Modal characteristics of conical shells have been studied by numerous investigators during the past ten years and computer programs are now available which enable one to compute the modes of a wide class of conical shells under general boundary conditions. An excellent summary of this work is contained in the papers by Hu[1] and Kalnins.[2] However, the principal contribution in each of these past studies has been the development of mathematical or numerical techniques for determining the modal characteristics, rather than a comprehensive study of the characteristics themselves. This paper presents results from an extensive study of the effects of shell geometry and boundary conditions on the axisymmetric modal characteristics of truncated conical shells. The study utilized the SABR1L computer code[3] which is an extensively modified version of the SABOR I computer code.[4] These programs are based on a finite-element method in which the shell is idealized as an assembly of conical shell frustum elements which are joined at nodal circles.

Discussion of Results

Figure 1 depicts a conical shell frustum. The semivertex angle α, the length parameter L/A, and the thickness parameter A/H, were varied to determine their effects on the axisymmetric modal behavior of the cone. Using the average cone radius A as a nondimensionalizing factor, values of the length parameter L/A are limited to the range $0 \leq L/A \leq 2 \csc\alpha$. The maximum value of L/A corresponds to a cone which is closed at its small end (i.e., a complete cone). Thin-shell theory is of course not applicable near the apex of a complete cone.

The SABR1L computer program used to generate the results of this study is based on Love's postulates and does not include the effects of rotatory inertia, shear deformations or transverse normal strains. Consequently shell modes such as thickness modes and thickness stretch modes that depend on the thickness coordinates are suppressed and only transverse and longitudinal motions are predicted. Based on information available for the spherical shell (see Ref. 5, Chap. 8), the SABR1L analysis should give good results for modes whose frequency ω is well below the frequency of the first thickness shear mode, that is

$$\omega \leq 0.1\omega_s \tag{1a}$$

In this expression ω_s may be approximated by the frequency of the lowest axisymmetric thickness shear mode for an infinite flat plate as obtained from an exact analysis within

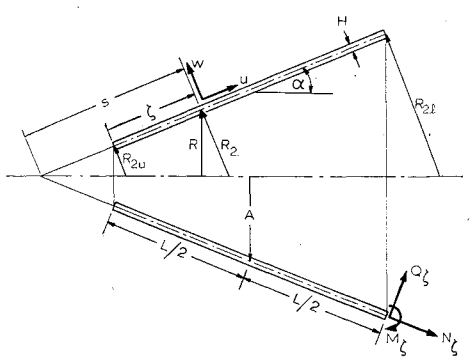

Fig. 1 Typical conical shell frustum.

Presented at the AIAA Structural Dynamics and Aeroelasticity Specialist Conference, New Orleans, La., April 16–17, 1969 (no paper number; published in bound volume of conference papers); submitted May 20, 1969; revision received May 22, 1970. This work was funded in part by the Lockheed Independent Research Program.

* Staff Scientist. Member AIAA.
† Research Scientist. Member AIAA.

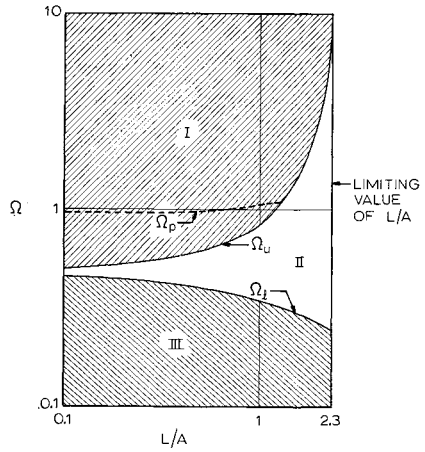

Fig. 2 Regimes on the frequency spectrum for a 60° cone.

the framework of the theory of elasticity. This frequency is given by the expression

$$\omega_s = (\pi/H)[E/2\rho(1 + \mu)]^{1/2} \quad (1b)$$

where μ = Poisson's ratio. For those modes which are primarily membrane in nature, the SABR1L analysis appears to give good results over an even broader range of frequencies because shear deformation and rotatory inertia are primarily associated with lateral deformation of the shell. The axisymmetric torsional modes were not considered. The five sets of boundary conditions listed in Table 1 were examined.

When analyzing cones that are very steep (nearly cylindrical), the concept of the "equivalent cylinder" is frequently introduced. The equivalent cylinder is one having its radius equal to the average radius of the cone and its length equal to the meridional length of the cone. The modal properties of the equivalent cylinder, which are relatively easy to obtain, are then taken as approximations to those of the steep cone. During this study, the validity of this approximation was examined.

Frequency Spectrum

Solutions to the linear differential equation system governing the axisymmetric free vibration of shells of revolution generally separate into two distinct classes. Four of the solutions are rapidly varying functions of the spatial coordinates and involve primarily bending of the shell wall. These are commonly referred to as bending solutions. The other two solutions are slowly varying functions of position and involve primarily stretching of the shell wall middle surface. These are the so-called membrane solutions. However, in a recent paper, Ross[6] has demonstrated that the governing system of

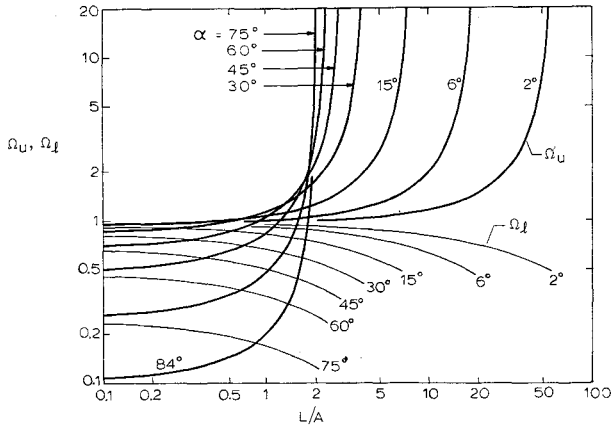

Fig. 3 Curves showing the effect of cone angle on the quantities Ω_u and Ω_l.

Table 1 Boundary conditions considered during the study

Case	Boundary conditions at $\zeta = 0$	Boundary conditions at $\zeta = L$
1	$w = 0,\ M_\zeta = 0,\ N_\zeta = 0$	$w = 0,\ M_\zeta = 0,\ N_\zeta = 0$
2	$w = 0,\ dw/d\zeta = 0,\ u = 0$	$w = 0,\ dw/d\zeta = 0,\ u = 0$
3	$M_\zeta = 0,\ N_\zeta = 0,\ Q_\zeta = 0$	$M_\zeta = 0,\ N_\zeta = 0,\ Q_\zeta = 0$
4	$w = 0,\ dw/d\zeta = 0,\ u = 0$	$M_\zeta = 0,\ N_\zeta = 0,\ Q_\zeta = 0$
5	$M_\zeta = 0,\ N_\zeta = 0,\ Q_\zeta = 0$	$w = 0,\ dw/d\zeta = 0,\ u = 0$

equations contain points in the neighborhood of which the solutions exhibit a strong interaction between bending and stretching effects. These are referred to as transition or turning points and they occur where

$$\omega_n^2 = E/\rho R_2^2$$

In this expression ω_n is the frequency of the nth normal mode, ρ and E are, respectively, the mass density and modulus of the shell, and R_2 is the circumferential radius of curvature as shown in Fig. 1. If a particular frequency lies in the interval

$$E/\rho R_{2l}^2 < \omega_n^2 < E/\rho R_{2u}^2 \quad (2)$$

where R_{2l} and R_{2u} are, respectively, the maximum and minimum values of R_2, then a transition point will occur for a value of $R_2 = [E/\rho\omega_n^2]^{1/2}$ which corresponds to a point on the cone. If $\omega_n^2 < E/\rho R_{2l}^2$ or $\omega_n^2 > E/\rho R_{2u}^2$, then the transition point occurs for a value of R_2 which does not correspond to a point on the cone.

In the following, we will discuss the frequency spectra for axisymmetric vibrations of conical shells. In these spectra, dimensionless frequency $\Omega = \omega/\omega_o$ is plotted as a function of L/A for fixed values of α and A/H. The constant ω_o is the frequency of a ring of radius A vibrating extensionally in plane strain

$$\omega_o = [E/\rho A^2(1 - \mu^2)]^{1/2}$$

It is convenient to divide the frequency spectra into three regimes defined by Eq. (2) as follows:
Regime I:

$$\Omega > \Omega_u = A(1 - \mu^2)^{1/2}/R_{2u} = \cos\alpha(1 - \mu^2)^{1/2}/(1 - L\sin\alpha/2A) \quad (3a)$$

Regime II:

$$\Omega_l \leq \Omega \leq \Omega_u \quad (3b)$$

Regime III:

$$\Omega < \Omega_l = A(1 - \mu^2)^{1/2}/R_{2l} = \cos\alpha(1 - \mu^2)^{1/2}/(1 + L\sin\alpha/2A) \quad (3c)$$

These regimes are illustrated for a 60° cone in Fig. 2. In regime II, the transition point occurs for a value of R_2 which corresponds to a point on the cone. In Fig. 3, the regimes defined by Eqs. (3) are plotted as functions of L/A for various values of the cone angle α. Note that Ω_u and Ω_l are independent of the thickness parameter A/H.

Axisymmetric frequency spectra for cones with both ends freely supported (case 1) and having semivertex angles of 5°, 45°, 60°, and 84° are shown in Fig. 4 for A/H equal to 20 and 500. For reference purposes, the frequency spectra for the cylinder ($\alpha = 0°$) and the annular plate ($\alpha = 90°$) are presented in Figs. 5 and 6. In all of these figures, the dimensionless frequency Ω is plotted as a function of L/A for approximately the first ten modes. Where the frequency curves intersect in Figs. 4–6, it was not possible to detect two distinct eigenvalues with the techniques used in this study.

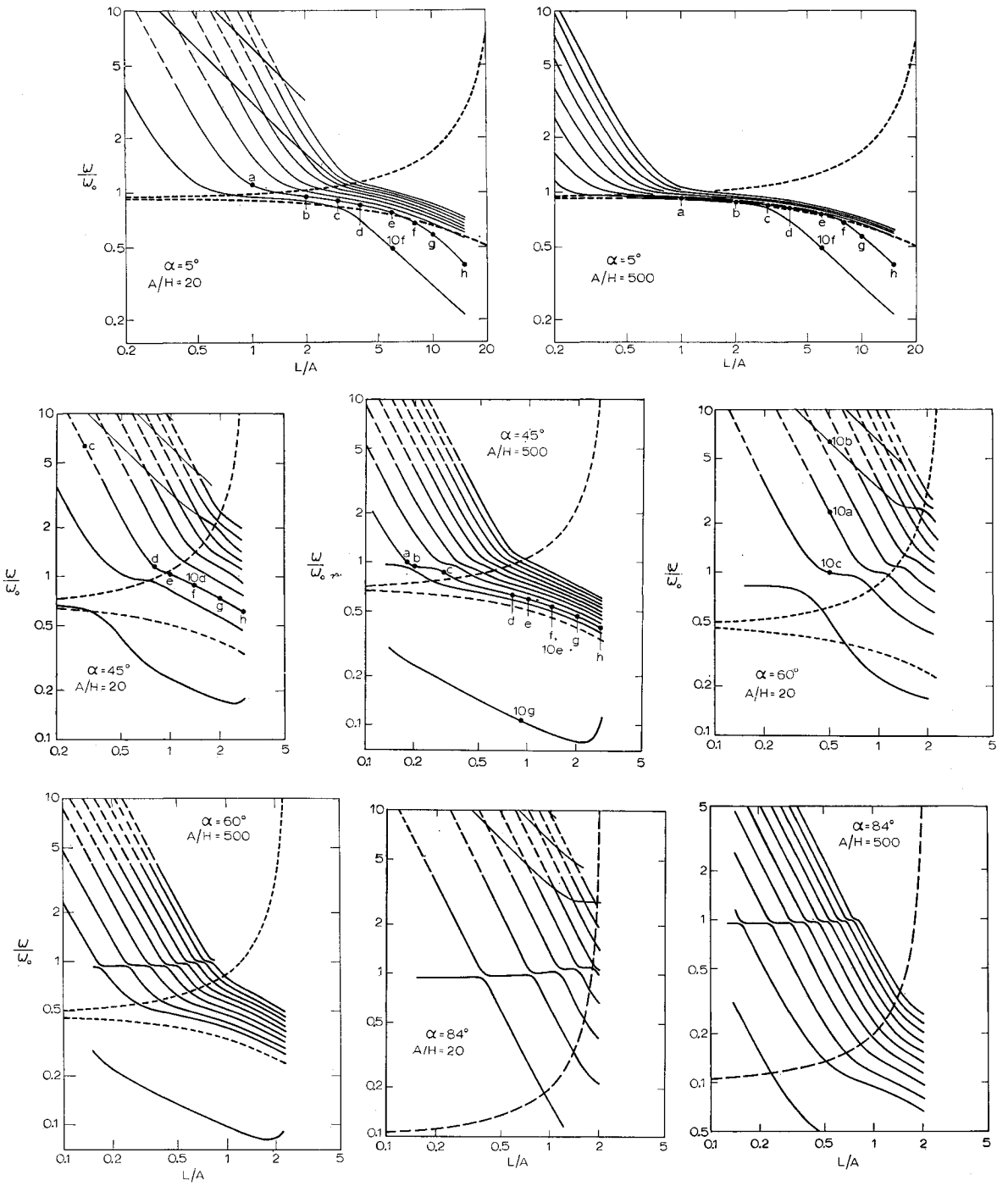

Fig. 4 Frequency spectrum for a freely supported (case 1) cone frusta with $A/H = 20$ and 500, for each of four half-angles.

Mode shapes corresponding to the points labeled 10a through 10g on the frequency spectra are shown as the corresponding pairs in Fig. 7.

In the frequency spectra shown in Fig. 4, regime I contains essentially two different families of curves. The modes corresponding to the steeper family involve primary lateral motion (see Fig. 7a) and these are referred to as lateral modes. Except in the vicinity of the I–II boundary, the characteristics of these modes are very similar to those of the lateral vibration of a uniform beam on an elastic foundation. As predicted by beam theory, these lateral modes are very sensitive to the thickness parameter and as the thickness increases the bending portion of the spectrum tends to shift to the right. For the modes that correspond to the other family of curves, the motion is predominantly longitudinal with a very small component in the lateral direction (see Fig. 7b). These modes are referred to as longitudinal modes and are quite insensitive to the thickness parameter. The characteristics of these longitudinal modes are very similar to those for the longitudinal vibration of a bar. It should be noted that curves for the longitudinal modes do not appear on the frequency spectra for the thin cones ($A/H = 500$) shown in Fig. 4, since the lower modes for these cones tend to be primarily lateral.

In regime I there are "kinks" in the lateral curves in the vicinity of the curve Ω_p. In this portion of the frequency spectrum the modes involve appreciable components of motion in both the lateral and longitudinal directions (see Figure 7c). In the limit as the cone angle approaches 90°, the kinked portions of the spectrum merge to form the curve Ω_p as shown in Figs. 2 and 6 and complete decoupling of lateral and longitudinal motion occurs as predicted by plate theory. Note that the extent of regime I increases with cone angle and that for $\alpha = 90°$ it occupies the entire spectrum.

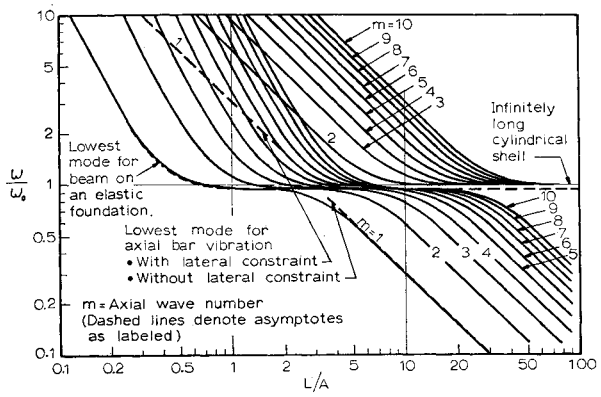

Fig. 5 Frequency spectrum for a freely supported (case 1) cylinder for $A/H = 20$.

As mentioned in the introduction, the effects of shear deformation and rotatory inertia are not included in the analysis used in this study. As a result, the analysis is unsuited for studying portions of the spectrum where these effects are important. Portions of the frequency spectra shown in Fig. 4 which do not satisfy the criterion of Eq. (1) are shown as dashed lines. In these regions, the effects of shear deformation and rotatory inertia should lower the frequencies.

It is in regime II that the novel feature of the modal behavior of the cone is exhibited. Here we find modes for which the large end of the cone vibrates vigorously while the small end remains relatively quiescent (see Fig. 7). In these modes significant components of both lateral and longitudinal motion are present, and the details of the mode shapes are strongly influenced by the thickness parameter and the location of the frequency within the regime. For thin cones and/or small cone angles, the frequency curves tend to be tightly spaced; while for thick cones and/or large cone angles, they are more widely spaced. Regardless of cone angle and thickness, the curves tend to run "parallel" to the lower boundary of regime II. As $\alpha \to 0$ regime II degenerates to the straight line $\Omega = (1 - \mu^2)^{1/2}$ while as $\alpha \to 90°$ it degenerates to the line $\Omega = 0$.

For the five sets of boundary conditions that have been considered in this study, there are (with two exceptions) no modes present in regime III for cone angles in excess of about 15°; and as $\alpha \to 90°$, the entire regime III disappears. As α decreases from 15°, modes begin to appear until there are infinitely many for the cylinder. All of these modes are primarily longitudinal and are approximated by the modes of a

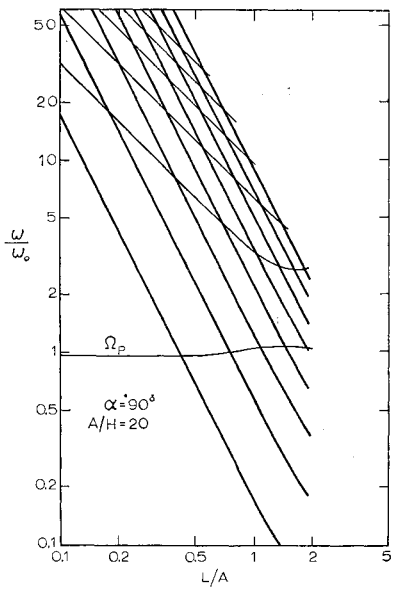

Fig. 6 Frequency spectrum for a freely supported (case 1) annular plate with $A/H = 20$.

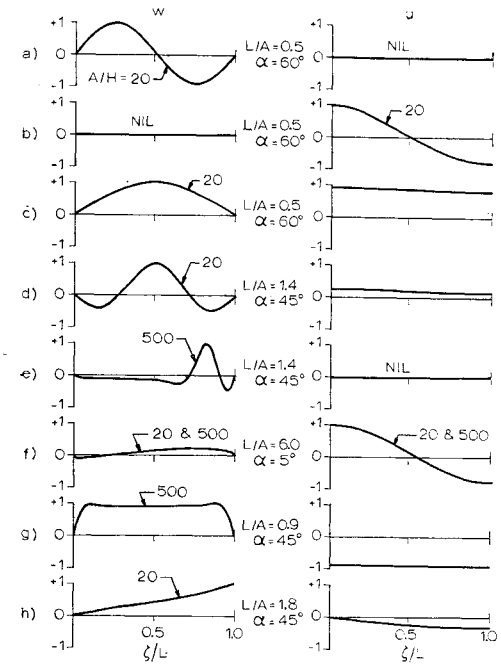

Fig. 7 Selected mode shapes for various cones with geometry as indicated. All are freely supported (case 1) except part h which is clamped-free (case 4).

bar vibrating longitudinally without lateral constraint. They are insensitive to the thickness parameter (see Fig. 7f). The exceptional cases mentioned previously occur for freely supported boundary conditions (case 1) and clamped-free boundary conditions (case 4). For case 1 there exists a mode which is most readily interpreted by recalling that the freely supported cylinder can move axially as a rigid body with zero frequency. Under these same boundary conditions however, the cone has its *axial* motion constrained even though its longitudinal motion is unconstrained since the directions of these motions differ by the cone semivertex angle. For small cone angles this constraint is small and a very low frequency axial mode results in which most of the cone moves as a rigid body

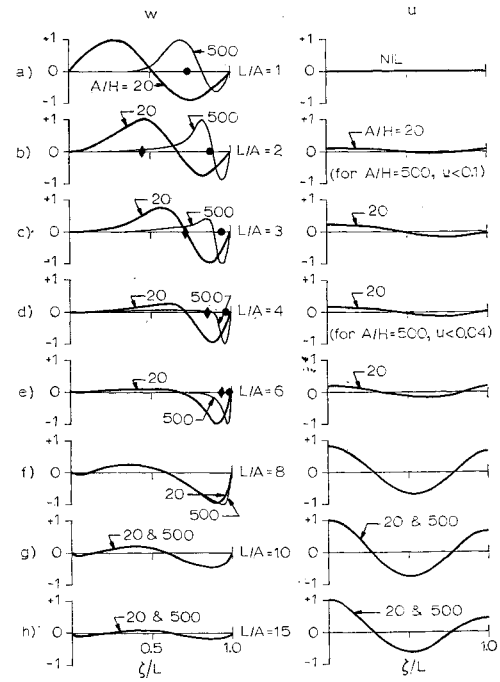

Fig. 8 Evolution of the third mode of a freely supported (case 1) 5° cone as L/A is varied.

with deformations occurring primarily in the immediate vicinity of the supports (see Fig. 7g). For the 5° cone, the frequency of this mode is too low to appear in Fig. 4, but for increasing α's up to 45°, this constraint increases and so does the frequency. As the cone angle increases beyond 45° the frequency begins to decrease until at 90° this mode becomes the lowest bending mode for an annular plate. For given values of the cone angle and L/A, the frequency of this mode increases with increasing values of the thickness parameter. Throughout the remainder of this paper, this mode will be referred to as a "quasi-rigid body mode."

The other exception occurs for case 4, where there is a low frequency "flapping mode" as shown in Fig. 7h. This mode involves considerable amounts of both tangential and normal motion.

Effect of Cone Length

Figures 8 and 9 illustrate the evolution of the third mode as L/A is varied for freely supported 5° and 45° cones, respectively, for A/H equal to 20 and 500. The points labeled alphabetically on the frequency curves (Fig. 4) correspond to the mode shapes labeled similarly in Figs. 8 and 9. For the 5° cone with $A/H = 20$, the frequency curve for the selected mode is well approximated by the frequency curve for the equivalent cylinder when L/A is less than about 1.0. Figure 8a shows that for $L/A = 1.0$, this mode involves primarily lateral motion, and the mode shapes differ only slightly from the simple sine and cosine which prevail for the corresponding mode of the equivalent cylinder. In Fig. 8b, we see that the normal displacement curve has the node occurring at $\zeta/L = 0.65$ and that the amplitude of the right-hand wave is equal to about 80% of the left-hand wave. Note that in moving from point a to point b on Fig. 4a we have moved into regime II, where the transition point corresponds to a point on the cone and where coupling between normal and longitudinal motion becomes significant. The location of the transition point is indicated by a diamond (or large dot for the case where $A/H = 500$) on the mode shapes shown in Figs. 8 and 9. In Figs. 8c–8e, the transition point moves toward the right-hand side of the cone, concentrating the normal motion there and causing the mode shapes to become increasingly distorted. In Fig. 8f, where the transition point has moved off of the right-hand end of the cone and we have entered

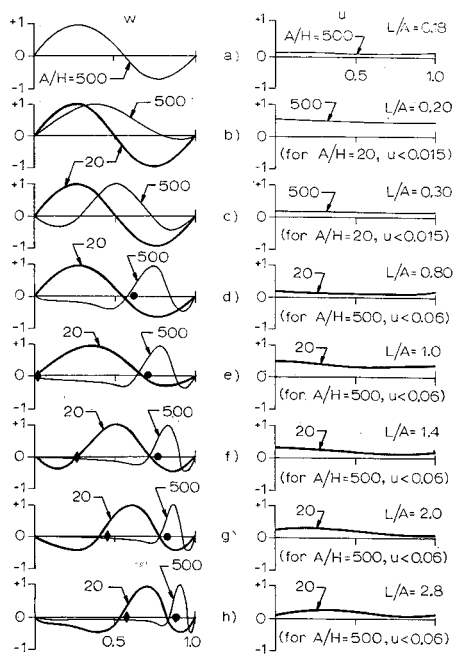

Fig. 9 Evolution of the third mode of a freely supported (case 1) 45° cone as L/A is varied.

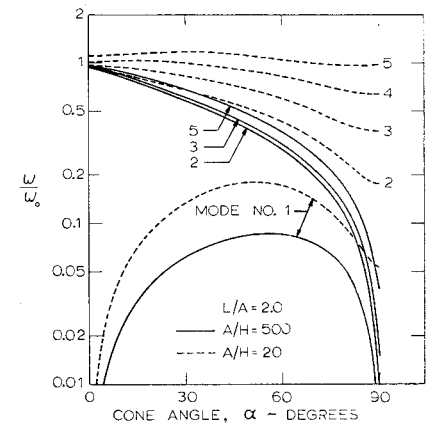

Fig. 10 Frequency vs cone angle for the first five modes of a freely supported cone (case 1).

regime III, the trend begins to change. While the normal motion is still dominant and distorted, the longitudinal motion becomes more significant and the mode shapes begin to resemble those of the equivalent cylinder again. In Fig. 11g, this new trend is further established until the longitudinal motion is clearly dominant for $L/A = 15$ (Fig. 8h).

Figure 8 also shows the mode shapes for the 5° cone with $A/H = 500$. For these cones, all modes that lie within regime II show more distortion than was evident with the thicker cones. Otherwise, the results are qualitatively the same as those for the thicker cones.

Consier next the mode shapes for the 45° cone, shown in Fig. 12. For the thin cone ($A/H = 500$), the modes for $L/A = 0.18$, 0.2, and 0.3 all lie within regime I (see Fig. 4). For $L/A = 0.18$ and 0.3, the motion is predominantly normal. However, for $L/A = 0.2$, the frequency is nearly on the Ω_p curve and as mentioned earlier, there is considerable coupling between the normal and the longitudinal motion of the cone as indicated by Fig. 9b. Note that in moving from Fig. 9a to 9c, the mode shape has changed its form considerably. For $L/A = 0.8$, we are now well within regime II and the distorted mode shapes characteristic of this regime are clearly evident in Figs. 9d–9g. For modes within regime II the large end of the cone tends to move normal to the meridian while the small end tends to move axially. This behavior is clearly illustrated by Fig. 9g, where, for $\zeta/L = 0.6$, both the normal and longitudinal displacements are equal to about 0.06, but they have opposite signs. Since $\alpha = 45°$, this means that the resultant motion is nearly axial. Finally, it should be noted that the strongly longitudinal modes which were observed in regime III for the 5° cone for larger values of L/A, are not present for the 45° cone.

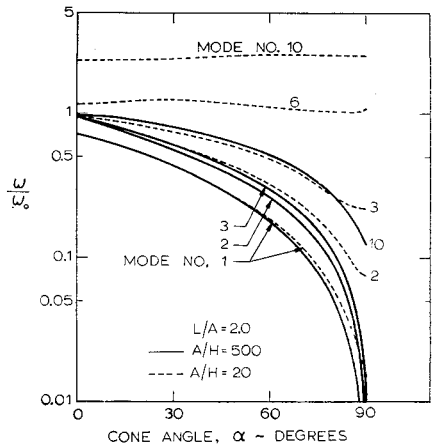

Fig. 11 Frequency vs cone angle for the first ten modes of a clamped-free cone (case 4).

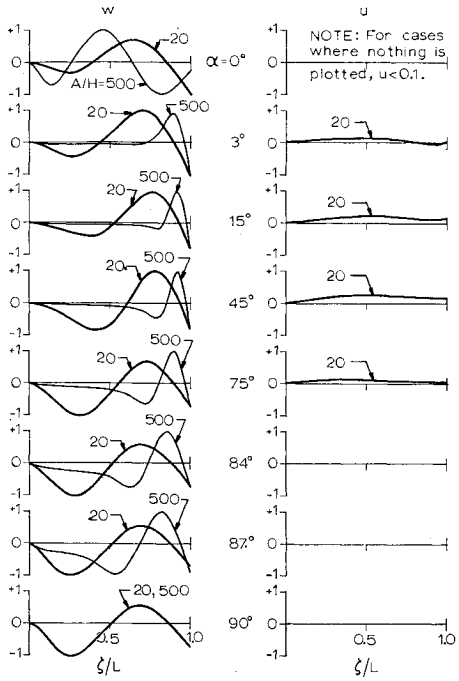

Fig. 12 Evolution of the third mode of a clamped-free (case 4) cone with increasing cone angle.

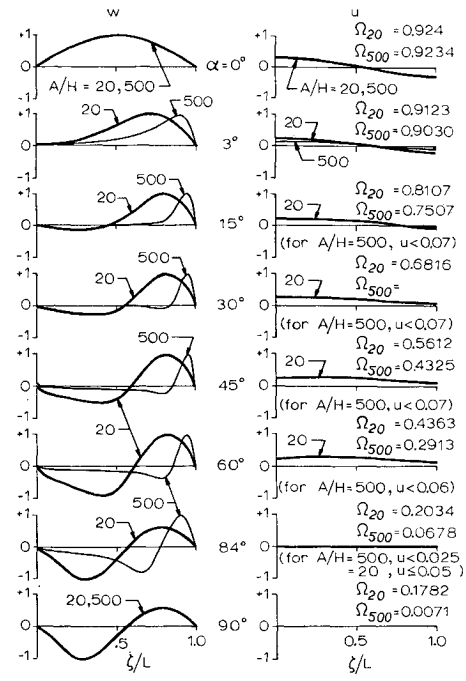

Fig. 13 Evolution of the second mode of a freely-supported (case 1) cone with increasing cone angle.

Variation of Modal Properties with Cone Angle

Figure 10 presents plots of frequency vs cone angle for the first five modes of a freely supported cone (case 1) with $L/A = 2$ and for $A/H = 20$ and 500. Figure 11 shows similar plots for the first ten modes of a clamped-free cone (case 4). Both of these plots indicate a generally downward shift in the frequency spectrum with increasing cone angle.‡ This effect is most pronounced with the lower modes and tends to disappear for progressively higher modes. The number of modes that are significantly dependent upon the cone angle is influenced by the thickness parameter A/H. Thus for the clamped-free cone, Fig. 11 indicates less than 10% variation in the frequency of the tenth mode for the entire range of α when $A/H = 20$, whereas for the thinner cone ($A/H = 500$) (there is a 90% variation in the frequency of this same mode over the same range of α. For a given α, the spacing between successive modes tends to increase with increasing thickness; for a given thickness, the spacing tends to increase with increasing α.

The accuracy with which the cone frequencies are approximated by the frequencies of the equivalent cylinder depends upon the cone angle as well as both the cone thickness and the particular mode under consideration. For example, for the freely supported cone with $A/H = 20$, the equivalent cylinder frequency approximates the frequency of the second cone mode to within 10% for cone angles up to 12°, while for the fifth mode the approximation is even better for the entire range of α. For the thinner cone with $A/H = 500$, the equivalent cylinder approximation is good to within 10% up to cone angles of about 9° for the second mode. For the fifth mode, it is good to 10% for $\alpha \leq 15°$. Regardless of thickness, the lowest mode of the freely supported cone is never well approximated by the lowest equivalent cylinder mode inasmuch as the cylinder mode is a rigid body mode with zero frequency.

For cases in which the cone is supported in the same manner at each edge (cases 1, 2, and 3), the frequency curves approach $\alpha = 0°$ with a horizontal slope. On the other hand, when each edge of the cone is supported in a different manner (cases 4 and 5), the frequency curves approach $\alpha = 0°$ with a finite slope (Figs. 10 and 11). The difference in behavior of the frequency curves near $\alpha = 0°$ for different boundary conditions tends to disappear for the higher modes.

For $L/A = 2$ and $A/H = 500$ and 20, the displacements associated with the third mode of a clamped-free cone and the second mode of a freely supported cone are shown, respectively, in Figs. 12 and 13 for various values of the cone angle. The frequency curves corresponding to these modes are contained in Figs. 10 and 11. It is interesting to note how drastically the mode shapes for the cone may differ from those of the equivalent cylinder even though the frequencies of the cone and the cylinder may be very close. In Fig. 13 we see that for $\alpha = 3°$ and $A/H = 500$, the frequency of the cone and the equivalent cylinder differ by only 2.26% whereas the mode shapes of the two are considerably different. The difference between the mode shapes is even more striking in Fig. 12 where again for $\alpha = 3°$ and $A/H = 500$ the frequencies differ by 4%. Figures 12 and 13 also illustrate that the modal behavior of a very flat thin cone ($\alpha = 87°$ for example) is very different from the modal behavior of an annular plate ($\alpha = 90°$). In this case both the frequency and the mode shape are significantly different.

Effect of Boundary Conditions

Most of the examples presented in this work involve cones with freely supported boundary conditions. Similar studies were made however for four other sets of boundary conditions (see Table 1). With the exception of the first few modes which are discussed in Ref. 7, no really significant differences in the modal behavior of the cone are observed for the various boundary conditions which were studied. In each case, the frequency curves tend to begin in regime I for small values of L/A where they are closely approximated by the frequency of an equivalent cylinder. Then they move into regimes II and III for the increasing values of L/A where differences between the modes obtained for cones with different boundary conditions tend to disappear.

Summary

This study of the axisymmetric modal properties of cone angle, cone length, and cone thickness demonstrated that

‡ In Fig. 13, the lowest quasi-rigid body mode is an exception to this statement.

these spectra could be considered to consist of three regimes defined by Eq. (3a–c). The character of any given mode is strongly dependent upon which of these regimes its frequency is contained in. A summary of the behavior of the cone in each regime is given below.

Regime I

Basically there are two types of modes present: one involves primarily *bending* of the shell wall, the other involves primarily *stretching* of the shell wall. For frequencies near that of the lowest in-plane vibration of an annular plate, a third type of mode involving both bending and stretching is present. The cone behaves very much like an equivalent cylinder with radius equal to the average radius of the cone and length equal to the meridian length of the cone. Frequencies and mode shapes for the equivalent cylinder closely approximate those of the cone. The effect of different boundary conditions and thickness on the cone can be assessed by examining their effect on the equivalent cylinder. As the cone half-angle α increases from 0° to 90°, the size of regime I increases until for 90° (an annular plate) it represents the entire frequency spectrum. However, except for influencing the size of the regime, α has little effect on the modes that lie in regime I.

Regime II

The transition point in the differential equations of motion corresponds to a physical point $[s = s_o = A(1 - \mu^2)^{1/2}/\Omega \tan\alpha]$ on the cone. The modes are characterized by *lateral* motion at the large end ($s > s_o$) of the cone and *axial* motion at the small end ($s < s_o$) of the cone. This phenomenon becomes more pronounced as the thickness of the cone is decreased. Even for very steep cones, these modes look quite different than those for the equivalent cylinder. Changing the boundary conditions at the large end of the cone has much more effect on the modal behavior than changing the boundary conditions at the small end. Increasing α tends to decrease the frequency of those modes contained in regime II. For a given L/A, decreasing the cone wall thickness tends to decrease the frequency of any given mode and to bring the frequencies of successive modes closer together.

Regime III

The degree to which modes having frequencies in regime III exist depends strongly on the cone angle and the boundary conditions. For $\alpha \gtrsim 15°$, there are (with two exceptions) no modes present in regime III for those boundary conditions investigated during this study. The two exceptions occur for the freely supported cone (case 1) where the quasi-rigid body mode is present and for the fixed-free cone (case 4) where flapping type mode exists. For $\alpha \lesssim 15°$, modes for which the motion is primarily longitudinal are also present. The number of these modes increases as α is decreased until for the cylinder ($\alpha = 0°$) there are infinitely many. These are well approximated by the equivalent cylinder. They are nearly independent of the thickness and only slightly affected by α. As α is increased from 0°, regime III decreases in size until for 90° it completely disappears.

The preceding summary applies to modes well within each of the regimes. Modes with frequencies that lie near the boundary between two regimes, tend to possess characteristics seen in each of these regimes.

References

[1] Hu, W. C. L., "A Survey of the Literature on the Vibrations of Thin Shells," TR 1, Southwest Research Institute Project 02-1504, 1964.

[2] Kalnins, A., "Dynamic Problems of Elastic Shells," *Applied Mechanics Review*, Vol. 18, No. 11, Nov. 1965, pp. 867–872.

[3] Loden, W. A., "SABR1L: A Finite Element Program for Static and Dynamic Analysis of Thin Shells of Revolution Under Axisymmetric Loading Conditions," Rept. B-21-67-8, Dec. 1967, Lockheed Missiles & Space Co., Palo Alto, Calif.

[4] Percy, J. H., Navaratna, D. R., and Klein, S., "SABOR I: A Fortran Program for the Linear Elastic Analysis of Thin Shells of Revolution Under Axisymmetric Loading by Using the Matrix Displacement Method," ASRL TR 121-5, April 1965, Massachusetts Institute of Technology, Cambridge, Mass.

[5] Kraus, H., *Thin Elastic Shells*, Wiley, New York, 1967.

[6] Ross, E. W., Jr., "Transition Solutions for Axisymmetric Shell Vibrations," *Journal of Mathematics and Physics*, No. 4, 1966, pp. 335–355.

[7] Hartung, R. F. and Loden, W. A., "Axisymmetric Vibration of Conical Shells," *Proceedings of AIAA Structural Dynamics and Aeroelasticity Specialist Conference*, AIAA, New York, 1969.